Comparative Toxicity of Nanoparticulate ZnO, Bulk ZnO, and ZnCl 2 to a Freshwater Microalga (Pseudokirchneriella subcapitata): The Importance of Particle Solubility

ARTICLE *in* ENVIRONMENTAL SCIENCE AND TECHNOLOGY · JANUARY 2008

Impact Factor: 5.33 · DOI: 10.1021/es071445r · Source: PubMed

6 AUTHORS, INCLUDING:

Graeme E Batley
Commonwealth Scientific and Industrial R…

218 PUBLICATIONS **7,469** CITATIONS

SEE PROFILE

Environ. Sci. Technol. **2007,** *41,* 8484–8490

Comparative Toxicity of Nanoparticulate ZnO, Bulk ZnO, and $ZnCl_2$ to a Freshwater Microalga (*Pseudokirchneriella subcapitata*): The Importance of Particle Solubility

NATASHA M. FRANKLIN,*,† NICOLA J. ROGERS,† SIMON C. APTE,† GRAEME E. BATLEY,† GERALD E. GADD,§ AND PHILIP S. CASEY‡

Centre for Environmental Contaminants Research, CSIRO Land and Water, Private Mail Bag 7, Bangor, NSW, Australia, 2234 CSIRO Manufacturing and Materials Technology, Clayton, Vic, Australia, 3168 Institute of Materials and Engineering Science, ANSTO, PMB 1, Menai, NSW, Australia, 2234

Received June 15, 2007. Revised manuscript received September 29, 2007. Accepted October 09, 2007.

Metal oxide nanoparticles are finding increasing application in various commercial products, leading to concerns for their environmental fate and potential toxicity. It is generally assumed that nanoparticles will persist as small particles in aquatic systems and that their bioavailability could be significantly greater than that of larger particles. The current study using nanoparticulate ZnO (ca. 30 nm) has shown that this is not always so. Particle characterization using transmission electron microscopy and dynamic light scattering techniques showed that particle aggregation is significant in a freshwater system, resulting in flocs ranging from several hundred nanometers to several microns. Chemical investigations using equilibrium dialysis demonstrated rapid dissolution of ZnO nanoparticles in a freshwater medium (pH 7.6), with a saturation solubility in the milligram per liter range, similar to that of bulk ZnO. Toxicity experiments using the freshwater alga *Pseudokirchneriella subcapitata* revealed comparable toxicity for nanoparticulate ZnO, bulk ZnO, and $ZnCl_2$, with a 72-h IC50 value near 60 μg Zn/L, attributable solely to dissolved zinc. Care therefore needs to be taken in toxicity testing in ascribing toxicity to nanoparticles per se when the effects may be related, at least in part, to simple solubility.

Introduction

Metal oxide nanoparticles are receiving increasing attention in materials science and nanotechnology-based industries for a large variety of applications, including catalysis, sensors, and environmental remediation, and for their incorporation into commercial products. In particular, nanoparticles such as ZnO and TiO_2 are being used in personal care products (e.g., sunscreens), and coatings and paints, on account of their UV absorption efficiency and transparency to visible light increases with decreasing particle size.

There is growing community and scientific concern that these desirable technological characteristics of nanoparticles may be offset by increased health and environmental risks, with the potential for exposure resulting in reactions at a cellular level that have not been observed with macroscopic materials. The small size of nanoparticles infers both greater mobility as well as potentially enhanced uptake across biological membranes (*1*). An increasing number of research articles have focused on the cytotoxicity of different types of engineered nanomaterials, with adverse effects suggested from exposure and uptake into mammalian cells, via the generation of reactive oxygen species (*2, 3*).

Much less is known about the environmental fate of nanomaterials and their potential toxicity to aquatic biota. Most work in this area has focused on fullerenes and, in particular, C_{60}, with reported effects including respiratory and growth inhibition of bacteria (*4, 5*), behavioral effects and acute mortality in water fleas (*Daphnia* species) (*6*), and cell damage in the brains of fish (*7*). There is still, however, disagreement in the actual mechanisms operating, and concerns have been made that the toxicity may be attributable to just residual solvent (*8*), and this is supported by later work showing dramatically reduced toxicity using water-stirred solubilization (*9*). There has also been a general lack of appropriate particle characterization (and reporting) in many ecotoxicological studies to date. Given the ability of nanoparticles to aggregate, studies that provide a nominal primary particle size alone (*10*) are likely to be inadequate for addressing specific nanoparticle risks. The degree of aggregation in a particular system being studied will strongly influence the availability of nanoparticles for uptake into cells (*11*). Similarly, nanoparticle morphology, surface area, surface charge, coating, purity, and its material solubility are expected to play very important roles in the fate and toxicity of the nanoparticles in aquatic systems. Given the well-known toxicity of the ionic forms of some metals (*12*), the solubility of metal and metal oxide nanoparticles may require particular attention. For example, it has been shown that the release of free cadmium from CdSe nanoparticles, rather than the nanoparticle itself, is responsible for cytotoxicity *in vitro* (*13*). Similarly, Brunner et al. (*14*) observed that material solubility strongly influenced the cytotoxic response of a range of oxide nanoparticles, with more soluble compounds like ZnO and FeO showing greater acute toxicity than nanoparticles of extremely low solubility such as CeO_2 and TiO_2.

To help elucidate the environmental fate and potential toxicity of ZnO nanoparticles, the present research has two aims. First, to characterize the fundamental properties of ZnO nanoparticles in a defined freshwater medium. Second, to assess the potential chronic toxicity of ZnO nanoparticles to the freshwater alga *Pseudokirchneriella subcapitata* by comparison to two reference toxicants, zinc chloride ($ZnCl_2$) and bulk ZnO of a non-nanoparticulate form.

Experimental Section

Nanoparticle Characterization Studies. Nanoparticulate ZnO was supplied from CSIRO Manufacturing and Materials Technology (Melbourne, Australia) with a nominal primary particle size of 30 nm. It was supplied in a powdered (nano-ZnO_{powder}) and an aqueous form (nano-$ZnO_{dispersant}$), with the latter containing 5% ZnO, 2% Teric N30 (Huntsman Corporation Australia Pty Ltd., Sydney, Australia), and 93% water.

* Corresponding author phone: +61 2 9710 6818; fax: +61 2 9710 6837; e-mail: Natasha.Franklin@csiro.au.
† CSIRO Land and Water.
§ ANSTO.
‡ CSIRO Manufacturing and Materials Technology.

 10.1021/es071445r CCC: $37.00
Published on Web 11/17/2007

Teric is a nonylphenol ethoxylate (NPE) that is commonly used as a surfactant and dispersing agent.

Concentrated suspensions of nanoparticulate ZnO (100 mg/L) were prepared and characterized using dynamic light scattering (DLS), transmission electron microscopy (TEM), and equilibrium dialysis. The concentration of ZnO chosen avoided a potential limitation in instrument detection by DLS and TEM and also ensured that excess zinc was present for the solubility experiments.

Dynamic Light Scattering (DLS). DLS measurements of nanoparticle suspensions were obtained using a high-performance particle sizer (Malvern Instruments Ltd., Worcestershire, U.K.). Appropriate amounts of nano-ZnO_{powder} or nano-$ZnO_{dispersant}$ were added to a synthetic freshwater algal medium, identical to that used for all algal bioassays. The low hardness and near-neutral pH of the medium was typical of natural freshwaters. All suspensions were vigorously shaken prior to analysis to break up visible clumps and resuspend any sedimented ZnO. The effect of employing a more thorough physical dispersion method on particle size distribution was assessed using an ultrasonicating probe (Daintree Scientific, St Helens, Australia; 2020XL; 60 W, 20 s duration).

Samples were placed in clean disposable cuvettes, and at least three consecutive measurements were performed at 25 °C, with each consisting of six runs of 20 s duration. Initially unfiltered suspensions were used to identify the entire particle size distribution. Samples were subsequently filtered through a 0.45 μm membrane filter to remove large particles that were interfering with the analysis. Samples that did not pass the instrument's internal quality criteria were disregarded.

Transmission Electron Microscopy (TEM). TEM (Philips CM100 operating at 80 kV) was used to visualize particle size and shape in subsamples of nanoparticle suspensions prepared in an identical manner to that outlined for DLS. Due to practical constraints, sonication and TEM sample preparation were undertaken 24 h prior to TEM analysis.

Samples were prepared by depositing a drop (6 μL) of the suspensions on a carbon-coated copper specimen grid and allowing the water to evaporate in a laminar flow hood. All sample analyses included at least four different magnifications (10 000, 25 000, 46 000, and 96 000) and at least five fields of view. TEM samples from aqueous medium blanks (no nanoparticles added) were included as controls.

Equilibrium Dialysis. Nanoparticle dissolution was assessed using Cole Parmer (Vernon Hills, IL) Spectra/Por 7 dialysis membranes of 1000 Da molecular weight cutoff (nominal pore size) and 45 mm diameter. The tubing was cut into 10 cm lengths and rinsed thoroughly in ultra-high-purity water (Milli-Q; Bedford, MA) prior to use. The dialysis cells were formed by filling the membrane tubes with Milli-Q water and sealing them with plastic dialysis clips which had been cleaned by soaking in 1% (v/v) nitric acid for several hours and thoroughly rinsed in Milli-Q water. The volume of the cells was approximately 10 mL.

Test solutions were prepared by adding nano-ZnO_{powder} (100 mg/L) to a 0.01 M $Ca(NO_3)_2$ solution in Milli-Q water buffered to pH 7.5 with 2 mM piperazine-N,N′-bis(ethanesulfonic acid) (PIPES; Sigma-Aldrich, St Louis, MO). This medium was chosen to minimize adsorptive losses of dissolved zinc onto container surfaces and to maintain the pH at 7.5 ± 0.15. Dialysis cells were added to the test solution and left to continually stir in a temperature- and light-controlled incubator used for the algal bioassays. To minimize dilution effects, care was taken to keep the volume of the dialysis cells below 5% of the total solution volume. At each sampling time, two cells were removed and sampled by pipet into polycarbonate vials. Samples of the external test solution were also taken at each time point for a measurement of pH and 0.1 μm filterable zinc. Total zinc in the test was measured at the start and end of the experiment only. Dialysis experiments were also performed in an identical manner with two reference compounds (analytical grade), bulk ZnO (Ajax Finechem, Sydney, Australia), and $Zn(NO_3)_2$ (BDH, Poole, U.K.). To identify the influence of zinc impurities from the ZnO powders on the dialyzed zinc fraction, additional samples of nano-ZnO_{powder} and bulk ZnO were repeatedly washed with Milli-Q water and oven-dried, and new suspensions (100 mg/L) were prepared and measured for dissolved zinc (0.1 μm filterable) over the same sampling period.

Algal Bioassays. The comparative toxicity of the various zinc compounds was assessed using *P. subcapitata* (formerly *Selenastrum capricornutum*) obtained from the American Type Culture Collection (Maryland, USA) and cultured axenically in a U.S. Environmental Protection Agency (EPA) medium (*15*) on a 24-h light cycle (Philips TL 40 W cool white fluorescent lighting, Danvers, MA, 70 μmol photons/m^2/s) at 24 °C.

The test medium was the standard U.S. EPA medium without ethylenediaminetetraacetic acid (*15*), prefiltered through a 0.22 μm membrane filter. The medium had an alkalinity of 9 mg of $CaCO_3$/L and a water hardness of 15 mg of $CaCO_3$/L. To minimize pH increases as a result of algal growth over 72 h, the medium was buffered with 2 mM PIPES to maintain the pH at 7.5 ± 0.1. Temperature and light conditions for the toxicity tests were identical to those used for culture maintenance. Tests solutions were continually shaken throughout the bioassay using a rotary shaker at 100 rpm.

Stock solutions (10, 50, and 100 mg/L) of bulk ZnO and $ZnCl_2$ (Sigma-Aldrich) were prepared in Milli-Q water. $ZnCl_2$ was used rather than $Zn(NO_3)_2$ to avoid potential nitrate nutrient supplementation. For $ZnCl_2$, the stocks were acidified to pH < 2 by the addition of Tracepur HCl (Merck, Darmstadt, Germany). Due to the amphoteric nature of ZnO, acidification of the stock was not carried out. For nano-ZnO_{powder} and nano-$ZnO_{dispersant}$, stock solutions were prepared in the buffered algal test medium (pH 7.5) to match the characterization studies. Controls, together with at least five contaminant concentrations (each in triplicate), were prepared with total zinc concentrations ranging from 25 to 600 μg Zn/L.

A total of 6 mL of toxicity test medium was dispensed into 30 mL borosilicate glass minivials, precoated with a silanizing solution (Coatasil, Ajax Finechem) to reduce the adsorption of dissolved zinc to the flask walls. All glassware was acid-washed in 10% concentrated HNO_3 and thoroughly rinsed with Milli-Q water before use. Additional minivials were prepared at each concentration for pH measurement at the beginning and end of the test and for determination of the total and dissolved (0.1 μm filterable) zinc.

Exponentially growing cells of *P. subcapitata* were harvested by centrifuging (700*g*, 7 min) and were washed three times with the test medium. Each minivial was inoculated with a known concentration of prewashed cells to give an initial cell density of $(1–2) \times 10^5$ cells/mL.

Algal cell counts were obtained using a four-color BD-FACSCalibur (Becton Dickinson BioSciences, San Jose, CA) flow cytometer as previously described by Franklin et al. (*16*). IC50 values (i.e., the inhibitory concentration giving a 50% reduction in algal growth rate after 72 h compared to the controls) were calculated using a linear interpolation method analysis (ToxCalc Version 5.0.23C, Tidepool Software, McKinleyville, CA). Tests of significance between the IC50 values were determined using the method described in Sprague and Fogels (*17*). Significance was tested at the $p = 0.05$ level.

Chemical Analysis. All samples for zinc analysis were acidified (0.2%) with Tracepur HNO_3 and measured by inductively coupled plasma−atomic emission spectrometry

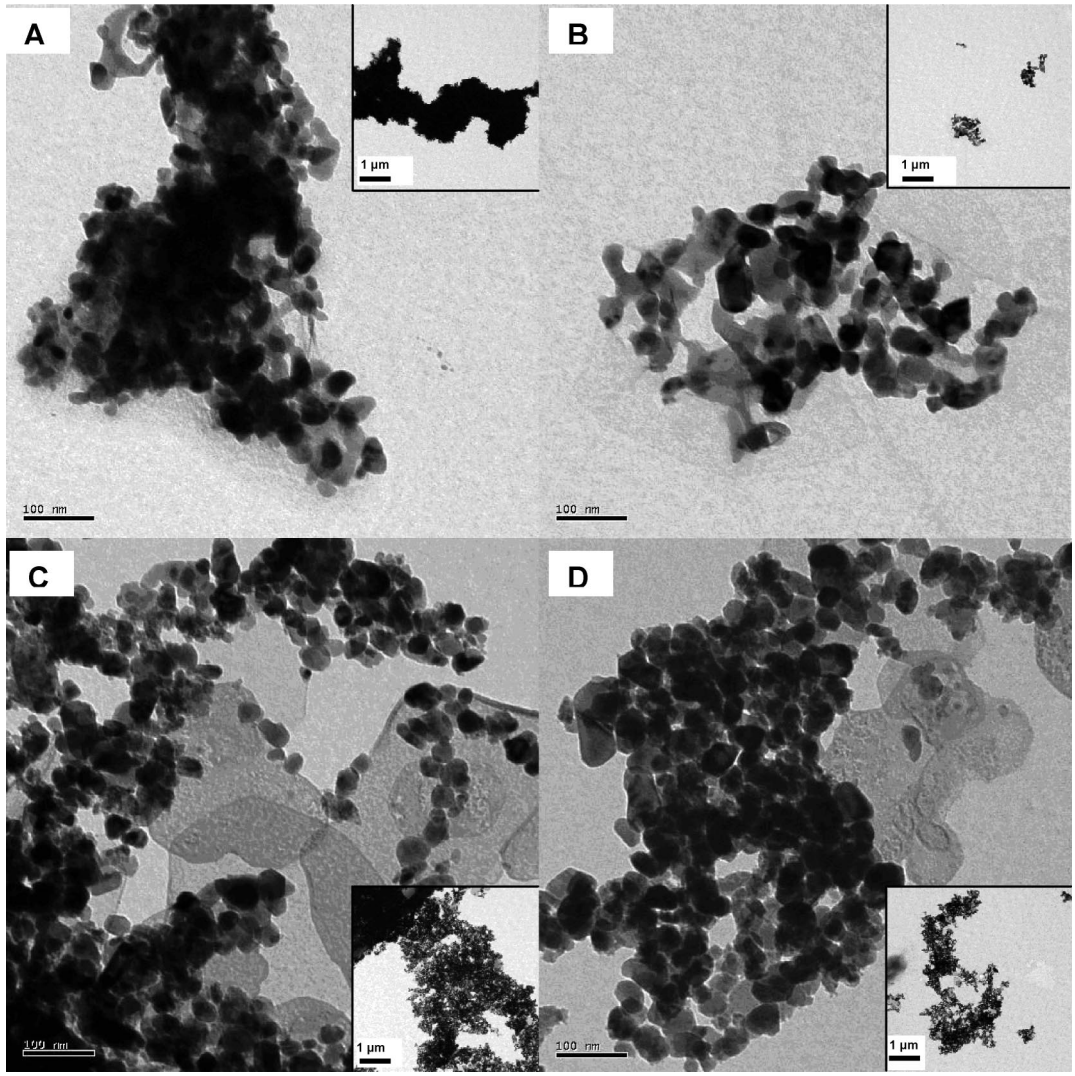

FIGURE 1. TEM images of ZnO nanoparticles (100 mg/L) in an algal test medium (pH 7.5). The inset picture illustrates the same sample but at a lower magnification: (a) unsonicated nano-ZnO_{powder}; (b) sonicated nano-ZnO_{powder}; (c) unsonicated nano-$ZnO_{dispersant}$; (d) sonicated nano-$ZnO_{dispersant}$.

(Spectroflame, EOP, Kleve, Germany). The instrument was calibrated using a mixed metal standard (QCD Analysts, diluted to 2 mg/L) and matrix-matched standards, and spike recovery samples were included in all analyses. The detection limit for zinc was 0.5 μg/L.

Results

Determination of Particle Size Distribution by TEM and DLS. TEM images of nano-ZnO_{powder} and nano-$ZnO_{dispersant}$ at concentrations of 100 mg/L are shown in Figure 1. Considerable particle aggregation was observed for each preparation (Figure 1a−d), resulting in the formation of flocs of variable sizes from a few hundred nanometers to several microns in diameter. Unsonicated nano-ZnO_{powder} (Figure 1a) appeared dense under TEM, indicating significant depth of the sample, and showed a general clumping to a few regions on the grid (Figure 1a, inset). The use of high-power sonication assisted in breaking up these larger flocs to smaller discrete aggregates (Figure 1b), although the primary particles were never isolated under the experimental conditions used. The nano-$ZnO_{dispersant}$ also showed aggregated ZnO particles (Figure 1c and d); however, unlike the powder alone, there were a small number of discrete particles. Dilution of this as-received nano-$ZnO_{dispersant}$ to 100 mg/L reduced the surfactant concentration from 2% to 0.004%, which may reduce its effectiveness in maintaining interparticle physical separation akin to the phenomenon of solvent shock. The effect of sonication was not as pronounced on the nano-$ZnO_{dispersant}$ with TEM images from samples prepared before and after sonication appearing very similar.

The primary ZnO nanoparticles observed by TEM were predominately near-spherical to ellipsoidal in shape. Apparent fusion of the primary particles was observed in some samples, although it was difficult to determine whether this was simply an artifact of the particles overlapping.

Using DLS, wide distributions of particle size were observed, all of which were considerably larger than the nominal size of 30 nm (Table 1), and in agreement with TEM measurements. The addition of nano-ZnO_{powder} to the aqueous medium resulted in visible flocs which settled within seconds. By contrast, a sonicated suspension of nano-ZnO_{powder} appeared cloudy and did not appear to settle over the sampling time. The particle size profiles of unfiltered nano-ZnO_{powder} suspensions typically showed two distinct populations, one with a mean peak of several hundred nanometers, and the presence of larger aggregates with a mean peak of several microns in diameter. Due to the strong influence of larger particles on the intensity-weighted size distribution of DLS measurements, samples were also filtered. This revealed a population of smaller particles (180–360 nm)

TABLE 1. Hydrodynamic Diameter of Nanoparticulate ZnO (100 mg/L, ca. 30 nm) in Algal Media (pH 7.5) Determined by Dynamic Light Scattering (T = 25 °C)

treatment		size range (nm)[a]
nano-ZnO_{powder}	unsonicated	particles settled out, failed QC[b]
	sonicated	565–3770
	sonicated, 0.45 μm filtered	178–361
nano-$ZnO_{dispersant}$	unsonicated	failed QC[a]
	sonicated	118–3140
	sonicated, 0.45 μm filtered	73–408

[a] On the basis of the intensity distribution or more than five separate measurements per sample. [b] QC: instrument defined quality criteria.

not previously observed in the unfiltered sample (Table 1). In the presence of a surfactant (nano-$ZnO_{dispersant}$), these smaller aggregates (100–400 nm) were typically observed without the need for filtering, due to them now comprising a greater proportion of the sample.

Determination of Nanoparticle Dissolution Using Dialysis. Figure 2 shows the dissolution of nanoparticulate ZnO powder compared to two reference materials, $Zn(NO_3)_2$ and bulk ZnO. Due to the extremely small nominal pore size (~1nm) of the dialysis membrane used, only the hydrated zinc ion or inorganic complexes of this size are able to pass through into the dialysis cell. For $Zn(NO_3)_2$, the diffusion of zinc into the dialysis cell was rapid, with equilibration attained within 6 h (Figure 2a).

The dissolution profiles from bulk ZnO and nanoparticulate ZnO are shown in Figure 2b and c, respectively. In addition to dialyzed zinc, measured filterable (0.1 μm) zinc (from the external solution) is also plotted, for suitable comparison purposes to zinc toxicity test results when only filtered (0.1 μm) samples could be obtained. At pH 7.6, rapid dissolution of the bulk ZnO and nanoparticulate ZnO was observed by 6 h, resulting in a dialyzed zinc concentration of approximately 8 mg/L, increasing to an equilibrium concentration of 16 mg of Zn/L after 72 h. This equates to 19% of the nominal total zinc concentration (100 mg/L). These results suggest that both the rate of dissolution and saturation solubility of ZnO are similar for bulk ZnO and nanoparticulate ZnO under these conditions. Given that, in our experimental system, the nanoparticulate ZnO dispersions were composed of aggregates of primary ZnO particles, only with information pertaining to freely dispersed ZnO primary particles can we make conclusions on how aggregation affects both the rate and extent of particle solubility.

Additional experiments on both washed and unwashed ZnO powder confirmed that soluble zinc impurities were not contributing to the measured dissolved zinc concentration (data not shown). Note that, because of the desire to discriminate both particulate and colloidal particles from those in true solution, our definition of "soluble" is based on the ability to pass through a dialysis membrane rather than the more usual 0.45 μm filtration.

Toxicity of Nanoparticulate ZnO, Bulk ZnO, and $ZnCl_2$ to *P. subcapitata*. The toxicity of the various zinc compounds to *P. subcapitata* is shown in Table 2. On the basis of total zinc concentrations, the chronic toxicity of nanoparticulate ZnO (nano-ZnO_{powder} and nano-$ZnO_{dispersant}$) was statistically similar (*17*) to that of bulk ZnO and $ZnCl_2$, resulting in 72-h IC50 values for growth inhibition ranging from 49 to 69 μg Zn/L. When expressed as dissolved zinc (0.1 μm filterable), similar concentration–response curves (data not shown) and corresponding 72-h IC50 values were obtained for each zinc compound (Table 2). All of the toxicity could be explained by the dissolved zinc. No toxicity was observed from the surfactant itself at the highest concentration of $ZnO_{dispersant}$ used (0.00125%); however, a significant inhibition of growth began to occur with only a 10-fold excess (e.g., ≥0.0125%).

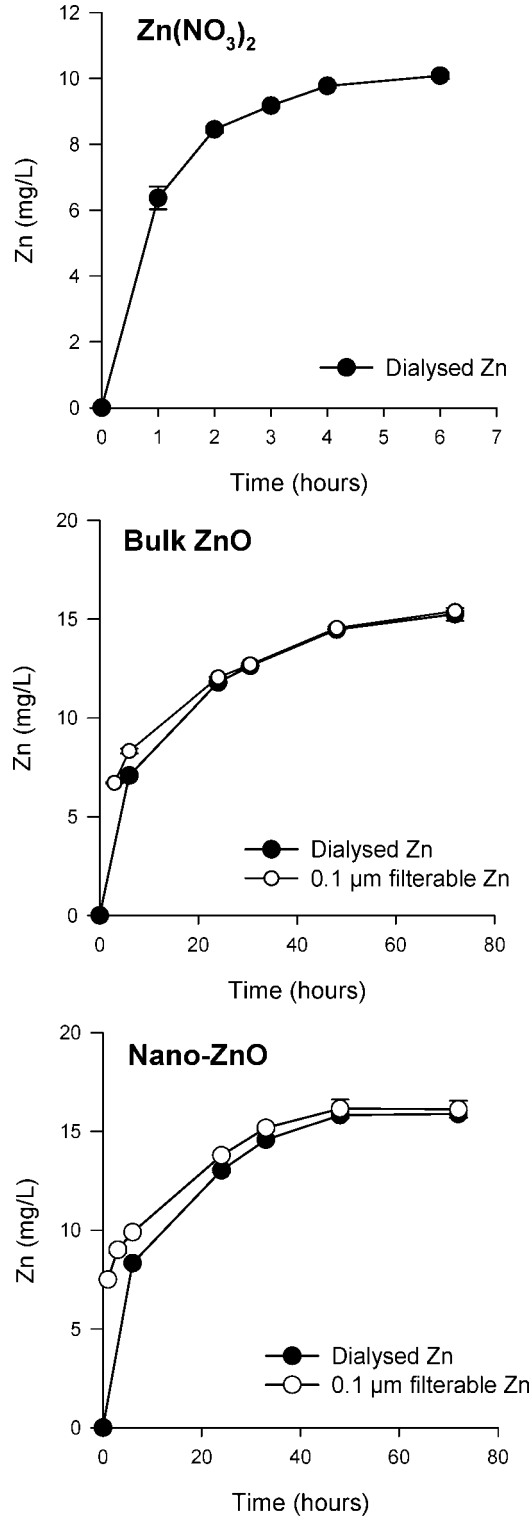

FIGURE 2. Determination of bulk ZnO and nanoparticulate ZnO dissolution rates by equilibrium dialysis, with comparison to dissolved $Zn(NO_3)_2$ solutions. Nominal total Zn concentration = 10 mg/L for $Zn(NO_3)_2$ and 100 mg/L for bulk and nanoparticulate ZnO. Values represent the mean ± SD of two samples. pH values for the $Zn(NO_3)_2$ experiment range from 7.40–7.50, bulk ZnO and nano-ZnO from 7.50–7.65.

TABLE 2. The 72-h IC50 (95% C.I) Values for *P. subcapitata* Exposed to $ZnCl_2$, Bulk ZnO, and Nanoparticulate ZnO, Expressed on the Basis of Dissolved Zn (0.1 μm filterable) Concentrations

	72-h IC50 values (μg/L)	
	total Zn	dissolved Zn
$ZnCl_2$	61 (38–74)	60 (44–69)
$ZnCl_2$ + surfactant	69 (51–85)	68 (52–81)
bulk ZnO	63 (36–84)	46 (24–66)
nano-ZnO_{powder}	68 (62–75)	68 (61–76)
nano-$ZnO_{dispersant}$	49 (41–65)	44 (36–62)

Discussion

Physical Characterization of Nanoparticles. Sound research on the ecotoxicity of nanoparticles requires appropriate characterization of the material and basic physicochemical information about the aqueous environment. Such information has been absent from many early studies, making it difficult to attribute specific effects to nanoparticulate materials per se. In aqueous systems, the solution pH and the presence of adsorbing molecules and ions will affect their surface charge and, hence, strongly influence aggregation behavior. At pH values closer to the isoelectric point (IEP), the charge on the particle is reduced and repulsive forces are lessened with aggregation expected to occur (*18*). An increase in electrolyte concentration however can induce aggregation of the particles at any pH (*18*), as observed in the case of C_{60} at ionic strengths greater than 0.05*I* (*4*). In natural waters, the presence of natural organic matter can also modify the surface charge of nanoparticles, leading to aggregation (*16*), as well as stabilizing nanoparticle suspensions through a combination of steric and electrostatic effects (*18, 19*).

The aggregation observed in our study has been reported elsewhere for ZnO (*20*) as well as for TiO_2 (*6*) and CeO_2 (*11*), in a range of aqueous conditions from distilled water to complex biological media, and is considered to be an inherent property of uncoated, nonmodified oxide nanoparticles (*14*). The inability to completely disperse particles by sonication suggests either irreversible fusion or strong bonding of the primary particles which cannot be broken apart by intense shear force, or a rapid reformation of the particles into aggregates after sonication. Despite the relatively low ionic strength of our medium, the solution pH likely played a key role in the aggregation behavior observed. For ZnO particles in aqueous solution, Degen and Kosec (*21*) report literature ranges for the IEP from pH 8.7 to 10.3, suggesting that pH 7.6 was unlikely to facilitate the formation of stable suspensions.

To overcome aggregation, commercial nanoparticle formulations often contain surfactants or capping agents to assist physical separation of the particles by maximizing the electrostatic repulsive force between charged particles, and by providing a barrier of steric hindrance. However, the very low concentrations of surfactant (NPE) used in our study did not result in dispersed suspensions of primary particles. At elevated surfactant concentrations, there is the possibility of toxicity from the surfactant itself (*22*), as well from possible synergistic interactions with the nanoparticles. In the environment, there are both naturally occurring (e.g., lactic acid and citrate) and anthropogenic surface modifiers (e.g., detergents), whose effects on the toxicity of nanoparticles warrant further attention.

Of the two techniques used to characterize the nanoparticles, TEM has the advantage of providing a direct image of particle size and morphology at high resolution (>0.1 nm spatial resolution); however, drawbacks include the need to use desiccated samples and ultra-high vacuum conditions, which may cause artifact formation. Alternative microscopy techniques such as environmental scanning electron microscopy or atomic force microscopy may be useful, as they allow imaging at closer to ambient conditions, although not without their own limitations (*23*). Caution should be employed in interpreting any microscopy results, and a statistically valid number of particles should be imaged to provide a good representation of the sample.

To complement microscopy techniques, DLS measured particle size in solution in real time with the advantage of needing little to no sample preparation (*24*). Due to the extensive aggregation of ZnO particles in the aqueous medium, the determination of particle size distribution by DLS was challenging and its ability to accurately characterize suspensions having a wide range of particle sizes was limited, since only a mean diameter and polydispersity index are provided. Nevertheless, DLS is a good choice when specifically examining whether nanoparticles have aggregated in solution.

Chemical Characterization of Nanoparticles. Understanding the aquatic chemistry of nanoparticles may also be important for aquatic toxicity investigations. Concerns about the bioavailability and toxicity of nanoparticulate materials arise from their assumed persistence as small particles in aquatic systems. In chemical data handbooks and material safety data sheets, ZnO (as well as many other metal oxides) is often classified as insoluble in water (*25*), when many are appreciably soluble (*26*). The aqueous solubility of ZnO is highly pH-dependent and reported to range from several thousand milligrams per liter at pH 6 to around 1 mg/L at pH 8 (*27*). At pH 7.6 in freshwater of moderate alkalinity, $Zn^{2+}_{(aq)}$ is the dominant species in solution, with a small contribution from $Zn(OH)^{+}_{(aq)}$ (*21*).

Using equilibrium dialysis, the equilibrium solubility of ZnO was determined as 16 mg/L (pH 7.6, 24 °C), higher than reported in the scientific literature (*27*); although, given that solution pH in this range has large effects on solubility, these differences are relatively small and not unexpected. The soluble zinc concentration was not due to zinc-containing impurities, as suggested by Degen and Kosec (*21*), since similar values were obtained after thoroughly washing the ZnO.

The rate of dissolution is considered proportional to particle surface area, and consequently nanoparticulate materials should dissolve faster than larger-sized bulk materials, for the same mass, on surface area considerations alone (*28*). Yang and Xie (*29*) showed that Zn^{2+} release rates from zinc and zinc oxide nanoparticles were faster than those from microparticles in the initial stages (<8 days) of the experiment. In addition to the kinetics of dissolution, the extent of particle solubility may also be size-dependent, with nanoparticles expected to have higher equilibrium solubility than macroscopic particles of the same material (*28, 30*). For liquid–solid systems, this relationship is described by the Ostwald−Freundlich equation (*28*). The dissolution of small particles involves a growth mechanism known as Ostwald ripening (*28*), with nanoparticle suspensions said to be unstable systems with solubility continuously changing with time (*31*). In addition to size and surface area, additional factors, such as surface curvature and roughness of the particle may play a role in the dissolution behavior (*28*). These phenomena challenge our traditional understanding of equilibrium solubility for micron-sized (bulk) materials and add additional complexity to working with nanosized materials.

The effect of particle size on dissolution rates was investigated by comparing bulk versus nanoparticulate ZnO. The results were not in agreement with the above theories, possibly due to the considerable aggregation observed in our experimental system. Exactly how aggregation affects the dissolution behavior of particles is not well understood.

The formation of clumps or clusters of primary particles (resulting in increased hydrodynamic size and reduced specific surface area) may hinder dissolution by reducing the average equilibrium solubility of the particle system and by introducing kinetic hindrance (*28*). The behavior may be further complicated by the aggregate volumes and packing factors, with larger, more densely packed aggregates exhibiting a slower dissolution (*28*).

Zinc Toxicity to Aquatic Organisms. Few researchers have considered the effect of particle solubility on the toxicity of nanoparticles, with most work centered on human health studies. For nanoparticulate metal oxides, Brunner et al. (*14*) recently highlighted the importance of particle solubility on the cytotoxic response of mammalian cell lines in vitro, with 3.75 mg/L of ZnO provoking a drop in cell functionality, attributed, at least in part, to a purely chemical effect of dissolved zinc ions. Unfortunately, no chemical measurements were made to quantify this relationship, nor were the pH values reported so that the extent of ZnO dissolution could be estimated. Given that the in vitro toxic concentrations of Zn^{2+} typically exceed 10 mg/L (*32*), the authors emphasized the difficulty in differentiating the effects of nanoparticulate ZnO from simple aqueous zinc species.

Aquatic organisms can be highly sensitive to dissolved zinc, so understanding the dissolution behavior of ZnO is critical in order to avoid a potential misinterpretation of results. Adams et al. (*20*) recommended the need for caution with nanomaterials, reporting that ZnO water suspensions were extremely toxic to *Daphnia magna* at concentrations as low as 0.2 mg/L (pH not reported). Significant (90%) growth inhibition was also reported for the bacterium *Bacillus subtilis*, albeit at a much higher ZnO concentration of 10 mg/L; however, given that this was the lowest concentration tested, impacts on growth presumably began at much lower ZnO concentrations. The authors did not consider the influence of dissolved zinc species on toxicity and attributed the effects solely to the nanoparticle suspensions. Given that these ZnO concentrations are well below the solubility limit obtained in our study, it is reasonable to suggest that toxicity may, at least in part, be related to zinc solubility. The inclusion of an appropriate reference material, for example, $ZnCl_2$, is unambiguously essential in order to assess specific nanoparticle risks.

Aquatic organisms display a broad range of sensitivities to zinc, although it is classified as an essential nutrient. Toxicity correlates best with the concentration of the free hydrated zinc ion (Zn^{2+}) or labile inorganic complexes, whereas zinc in strong complexes, or adsorbed to colloidal and particulate matter, has a low bioavailability (*12*). The acute toxicity of zinc to various invertebrates and fish has been reported from to be 40 μg/L to 58 mg/L, with toxicity dependent on water hardness (*33*). The algal growth rate is sensitive to dissolved zinc, with reported EC50 values as low as 40 μg Zn/L for *Chlorella vulgaris* and *Raphidocelis subcapitata* (*34, 35*). Furthermore, significant fish mortality (30-day LOEC: 28 μg Zn/L) (*36*) and impaired reproduction of daphnids (i.e., 21-day EC50: 91 μg Zn/L based on net reproductive rate) (*37*) have also been noted at comparatively low dissolved zinc concentrations.

Environmental Relevance of ZnO Nanoparticles. The principal concern associated with the release of nanomaterials is how their smaller particle size may alter the materials transport, fate, and potential toxicity to aquatic organisms compared to larger particles. For ZnO, we observed no size-related effects; rather, the most likely impact of ZnO (nanoparticulate or bulk) resulted from dissolution presumably as Zn^{2+} or small inorganic complexes which are highly toxic to a range of aquatic organisms. This process is not limited to aquatic systems but may equally apply to soil environments, where pH strongly affects the dissolution, and ZnO is also considered too soluble to persist in soils (*38*). The issue of photoinduced ZnO toxicity (as a result of UV-A radiation) was not considered in the present study due to the rapid dissolution of the ZnO particles in our test media. This resulted in immediate dissolved Zn concentrations well in excess of the IC50 value for this species, likely precluding additional mechanisms of toxicity, such as photocatalytic effects. However, the dissolution behavior and potential phototoxicity of other nanomaterials needs to be individually assessed to determine their specific risks. For less soluble materials, dissolution over a longer time frame of weeks to months may become significant to their persistence in the environment and ultimate toxicity.

Acknowledgments

We are grateful to Barbara Bojarski, CSIRO Molecular and Health Technologies, for the TEM analysis.

Literature Cited

(1) Chithrani, B. D.; Ghazani, A. A.; Chan, W. C. Determining the size and shape dependence of gold nanoparticle uptake into mammalian cells. *Nano. Lett.* **2006**, *6*, 662–668.
(2) Sayes, C. M.; Gobin, A. M.; Ausman, K. D.; Mendez, J.; West, J. L.; Colvin, V. L. Nano-C_{60} cytotoxicity is due to lipid peroxidation. *Biomaterials* **2005**, *26*, 7587–7595.
(3) Long, T. C.; Saleh, N.; Tilton, R. D.; Lowry, G. V.; Veronesi, B. Titanium dioxide (P25) produces reactive oxygen species in immortalized brain microglia (BV2): Implications for nanoparticle neurotoxicity. *Environ. Sci. Technol.* **2006**, *40*, 4346–4352.
(4) Fortner, J. D.; Lyon, D. Y.; Sayes, C. M.; Boyd, A. M.; Falkner, J. C.; Hotze, E. M.; Alemany, L. B.; Tao, Y. J.; Guo, W.; Ausman, K. D.; Colvin, V. L.; Hughes, J. B. C_{60} in water: Nanocrystal formation and microbial response. *Environ. Sci. Technol.* **2005**, *39*, 4307–4316.
(5) Lyon, D. Y.; Fortner, J. D.; Sayes, C. M.; Colvin, V. L.; Hughes, J. B. Bacterial cell association and antimicrobial activity of a C_{60} water suspension. *Environ. Toxicol. Chem.* **2005**, *24*, 2757–2762.
(6) Lovern, S. B.; Kapler, R. *Daphnia magna* mortality when exposed to titanium dioxide and fullerene (C_{60}) nanoparticles. *Environ. Toxicol. Chem.* **2006**, *25*, 1132–1137.
(7) Oberdörster, E. Manufactured nanomaterials (fullerenes, C_{60}) induce oxidative stress in the brain of juvenile largemouth bass. *Environ. Health Perspect.* **2004**, *112*, 1058–1062.
(8) Andrievsky, G.; Klochkov, V.; Derevyanchenko, L. Is the C_{60} fullerene molecule toxic. *Fullerenes, Nanotubes, Carbon Nanostruct.* **2005**, *13*, 363–376.
(9) Zhu, S.; Oberdörster, E.; Haasch, M. L. Toxicity of an engineered nanoparticle (fullerene, C_{60}) in two aquatic species *Daphnia* and fathead minnow. *Mar. Environ. Res.* **2006**, *62*, S5–S9.
(10) Hund-Rinke, K.; Simon, M. Ecotoxic effect of photocatalytic active nanoparticles (TiO_2) on algae and daphnids. *Environ. Sci. Pollut. Res.* **2006**, 1–8.
(11) Limbach, L. K.; Yuchun, L.; Grass, R. N.; Brunner, T. J.; Hintermann, M. A.; Muller, M.; Gunther, D.; Stark, W. J. Oxide nanoparticle uptake in human lung fibroblasts: Effects of particle size, agglomeration, and diffusion at low concentrations. *Environ. Sci. Technol.* **2005**, *39*, 9370–9376.
(12) Campbell, P. G. C. Interactions between trace metals and aquatic organisms: a critique of the free-ion activity model. Metal Speciation and Bioavailability in Aquatic Systems; Tesser, A., Turner, D. R., Eds.; In John Wiley and Sons: Chichester, West Sussex, U.K., 1995; pp 45−102.
(13) Derfus, A. M.; Chan, W. C. W.; Bhatia, S. N. Probing the cytotoxicity of semiconductor quantum dots. *Nano. Lett.* **2004**, *4*, 11–18.
(14) Brunner, T. J.; Wick, P.; Manser, P.; Spohn, P.; Grass, R. N.; Limbach, L. K.; Bruinink, A.; Stark, W. J. In vitro cytotoxicity of oxide nanoparticles: Comparison to asbestos, silica, and the effect of particle solubility. *Environ. Sci. Technol.* **2006**, *40*, 4374–4381.
(15) *Short-term Methods for Estimating the Chronic Toxicity of Effluents and Receiving Waters to Freshwater Organisms*, 3rd ed.; United States Environment Protection Agency Report EPA-600-4-91-002, U.S. EPA: Cincinnati, OH, 1994; pp 341.
(16) Franklin, N. M.; Stauber, J. L.; Lim, R. P. Development of multispecies algal bioassays using flow cytometry. *Environ. Toxicol. Chem.* **2004**, *23*, 1452–1462.

(17) Sprague, J. B.; Fogels, A. Watch the Y in bioassay. *Proceedings Third Aquatic Toxicity Workshop*,Halifax, Nova Scotia, November 2–3, 1976; pp 107–114.
(18) Illés, E.; Tombácz, E. The effect of humic acid adsorption on pH-dependent surface charging and aggregation of magnetite nanoparticles. *J. Colloid Interface Sci.* **2006**, *295*, 115–123.
(19) Hyung, H.; Fortner, J. D.; Hughes, J. B.; Kim, J.-H. Natural organic matter stabilizes carbon nanotubes in the aqueous phase. *Environ. Sci. Technol.* **2007**, *41*, 179–184.
(20) Adams, L. K.; Lyon, D. Y.; McIntosh, A.; Alvarez, P. J. J. Comparative toxicity of nano-scale TiO_2, SiO_2 and ZnO water suspensions. *Water Sci. Technol.* **2006**, *54*, 327–334.
(21) Degen, A.; Kosec, M. Effect of pH and impurities on the surface charge of zinc oxide in aqueous solution. *J. Eur. Ceram. Soc.* **2000**, *20*, 667–673.
(22) Xia, W. J.; Onyuksel, H. Mechanistic studies on surfactant-induced membrane permeability enhancement. *Pharm. Res.* **2000**, *17*, 612–618.
(23) Lead, J. R.; Wilkinson, K. J. Aquatic colloids and nanoparticles: Current knowledge and future trends. *Environ. Chem.* **2006**, *3*, 159–171.
(24) Burleson, D. J.; Driessen, M. D.; Penn, R. L. On the characterization of environmental nanoparticles. *J. Environ Sci. Health* **2004**, *A39*, 2707–2753.
(25) *Handbook of Chemistry and Physics Online*, 87th ed.; CRC Press: Boca Raton, FL, 2006–2007.
(26) Rogers, N. J.; Franklin, N. M.; Apte, S. C.; Batley, G. E. The importance of physical and chemical characterization in nanoparticle toxicity studies. *Integr. Environ. Assess. Manage.* **2007**, *3*, 7–8.
(27) Stumm, W.; Morgan, J. J. Aquatic Chemistry. *Chemical Equilibria and Rates in Natural Waters*, 3rd ed.; Wiley-Interscience: New York, 1995.
(28) Borm, P.; Klaessig, F. C.; Landry, T. D.; Moudgil, B.; Pauluhn, J.; Thomas, K.; Trottier, R.; Wood, S. Research strategies for safety evalulation of nanomaterials, Part V: Dissolution in biological fate and effects of nanoscale particles. *Toxicol. Sci.* **2006**, *90*, 23–32.
(29) Yang, Z.; Xie, C. Zn^{2+} release from zinc and zinc oxide particles in simulated uterine solution. *Colloids Surf., B* **2006**, *47*, 140–145.
(30) Roelofs, F.; Vogelsberger, W. Dissolution kinetics of synthetic amorphous silica in biological-like media and its theoretical description. *J. Phys. Chem. B* **2004**, *108*, 11308–11316.
(31) Rickard, D.; Morse, J. W.; Luther, G. W. Clusters, nanoparticles and the solubility constant. *Abstracts for Goldschmidt*,Copenhagen, Denmark, June 5–11, 2004.
(32) Palmiter, R. D. Protection against zinc toxicity by metallothionein and zinc transporter 1. *Proc. Natl. Acad. Sci. U.S.A.* **2004**, *101*, 4918–4923.
(33) *Zinc Oxide; Toxic Chemical Release Reporting; Community Right-To-Know*; United States Environment Protection Agency: Cincinnati, OH, 1995;Federal Register, *60* (176), 47334–47337.
(34) Muyssen, B. T. A.; Janssen, C. R. Zinc acclimation and its effect on the zinc tolerance of *Raphidocelis subcapitata* and *Chlorella vulgaris* in laboratory experiments. *Chemosphere* **2001**, *45*, 507–514.
(35) Franklin, N. M.; Adams, M. S.; Stauber, J. L.; Lim, R. P. Development of an improved rapid enzyme inhibition bioassay with marine and freshwater microalgae using flow cytometry. *Arch. Environ. Contam. Toxicol.* **2001**, *40*, 469–480.
(36) Woodling, J.; Brinkman, S.; Albeke, S. Acute and chronic toxicity of zinc to the mottled sculpin *Cottus bairdi*. *Environ. Toxicol. Chem.* **2002**, *21*, 1922–1926.
(37) Muyssen, B. T. A.; Janssen, C. R. Importance of acclimation to environmentally relevant zinc concentrations on the sensitivity of *Daphnia magna* toward zinc. *Environ. Toxicol. Chem.* **2005**, *24*, 895–901.
(38) Lindsay, W. L. *Chemical Equilibria in Soils*; John Wiley and Sons: New York, 1979.

ES071445R